

# Contributions to the event-by-event charge asymmetry dependence for the elliptic flow of $\pi^+$ and $\pi^-$ in heavy-ion collisions

Adam Bzdak\*

*RIKEN BNL Research Center,  
Brookhaven National Laboratory,  
Upton, NY 11973, USA*

Piotr Bożek†

*AGH University of Science and Technology,  
Faculty of Physics and Applied Computer Science, PL-30-059 Kraków, Poland  
Institute of Nuclear Physics, PL-31342 Kraków, Poland*

## Abstract

We discuss various contributions to the event-by-event charge-asymmetry dependence of  $\pi^+$  and  $\pi^-$  elliptic flow, recently measured by the STAR Collaboration at RHIC. It is shown that under general assumptions, the difference between  $v_2^+$  and  $v_2^-$  at a given fluctuating value of an asymmetry parameter,  $A$ , is a linear function of  $A$ , as observed in the preliminary data. We discuss two mechanisms that are qualitatively consistent with the experimental data and result in a signal of the correct order of magnitude. Our subsequent hydrodynamic calculations, assuming local charge conservation at freeze-out, yield a qualitative and partial quantitative understanding of the observed signal, so offering a detailed test of the hydrodynamic model in heavy-ion collisions.

---

\*Electronic address: [abzdak@bnl.gov](mailto:abzdak@bnl.gov)

†Electronic address: [piotr.bozek@ifj.edu.pl](mailto:piotr.bozek@ifj.edu.pl)

## I. INTRODUCTION

Recent experimental measurements of elliptic anisotropy have challenged the conventional hydrodynamic picture of relativistic heavy-ion collisions that had proven very effective in facilitating our understanding of many features of particle production in such collisions [1–3].

For instance, as reported in Ref. [4], at a given energy and centrality of a collision the elliptic flow for particles and antiparticles is slightly different. In particular the elliptic flow for protons is larger than for antiprotons, and the difference between the two decreases with increasing energy. This effect can be understood either as a result of baryon stopping [5, 6] or by including the mean-field potentials in the hadronic phase, as shown in the AMPT model [7].

An intellectually more challenging experimental observation is the dependence of elliptic flow for  $\pi^+$  and  $\pi^-$  as a function of the event-by-event fluctuating asymmetry parameter,

$$A = \frac{N_+ - N_-}{N_+ + N_-}, \quad (1.1)$$

where  $N_+$  and  $N_-$  denote, respectively, the numbers of positively and negatively charged particles at a given acceptance region. According to the preliminary STAR data [8, 9], at a certain energy and centrality class, the elliptic flow for  $\pi^+$  is a decreasing function of  $A$ , and, for  $\pi^-$ , the opposite trend is observed. In particular

$$\langle v_2^- \rangle_A - \langle v_2^+ \rangle_A = c + rA, \quad (1.2)$$

where  $\langle v_2 \rangle_A$  denotes an average elliptic flow at a given value of  $A$ , and  $c$  and  $r$  are parameters. The preliminary STAR data shows that in Au+Au mid-peripheral collisions at various energies  $r_{\text{exp}} \approx 0.03$  [8, 9], where both  $A$  and  $v_2$  are measured in  $|\eta| < 1$ .

As shown in [10], this dependence cannot be understood in the baryon- (or isospin-) stopping scenario. Moreover, both UrQMD [11] and AMPT [12] models fail to describe the linear relation (1.2) [8]. Recently, an interesting interpretation of Eq. (1.2) was proposed as evidence of the effects of a chiral magnetic wave [13–15]. This effect is closely related to the chiral magnetic effect [16], discussed extensively in the recent literature, e.g., the recent review in [17].

In this paper, we demonstrate that Eq. (1.2) is consistent with the hydrodynamic picture of heavy-ion collisions with local charge conservation at freeze-out. We discuss the relation between Eq. (1.2) and the physics underlying the charge balance function [18], successfully described by hydrodynamic models, e.g., [19, 20]. In the following section, we derive a general relation between  $\langle v_2^\pm \rangle_A$  and  $A$ , yielding a linear dependence. In section 3, we discuss two mechanisms that qualitatively and partly quantitatively reproduce the experimental data. In section 4, we detail state-of-the-art 3 + 1-dimensional hydrodynamic calculations with local charge conservation, observing a strong signal consistent with the experimental one, within a factor of 2. Section 5 gives our comments and conclusions.

## II. GENERAL RELATIONS

In this section we derive the relation between elliptic flow at a given  $A$ ,  $\langle v_2 \rangle_A$ , as a function of  $\langle v_2 \rangle_{A=0}$  and  $A$ . Here, for simplicity, we assume that the distribution of  $A$  at a

given centrality class is symmetric with respect to  $A = 0$ .<sup>1</sup>

Straightforwardly, we notice that for a sufficiently small  $A$

$$\langle N_+ - N_- \rangle_A = \alpha A \langle N_+ + N_- \rangle_{A=0} = 2\alpha A \langle N_+ \rangle_{A=0}, \quad (2.1)$$

where  $\alpha$  is a parameter whose value is close to unity<sup>2</sup>, see Eq. (1.1). Here,  $\langle \cdot \rangle_{A=0}$  denotes an average over all events characterized by  $A = 0$ . We readily notice that

$$\langle N_+ + N_- \rangle_A = 2 \langle N_+ \rangle_{A=0} (1 - \beta^2 A^2 + \dots). \quad (2.2)$$

The left-hand side of the above equation is invariant under the transformation  $A \rightarrow -A$ ; thus, only the even powers of  $A$  are allowed.<sup>3</sup> These equations above support our evaluation of  $\langle N_+ \rangle_A$  and  $\langle N_- \rangle_A$

$$\langle N_{\pm} \rangle_A = \langle N_+ \rangle_{A=0} (1 \pm \alpha A - \beta^2 A^2 + \dots). \quad (2.3)$$

To express elliptic flow at a given  $A$  as a function of  $A$  we write

$$\left\langle \frac{d^3 N_+}{d\varphi d^2 p_t} \right\rangle_A = \left\langle \frac{d^3 N_+}{d\varphi d^2 p_t} \right\rangle_{A=0} + \left\langle \frac{d^3 N_+}{d\varphi d^2 p_t} \right\rangle_{\text{asym}}, \quad (2.4)$$

and analogously for negative particles. Here,  $\langle \cdot \rangle_{\text{asym}}$  represents an average number of particles responsible for a non-zero value of  $A$ . Integrating the above equation over  $\varphi$  and  $p_t$  we obtain Eq. (2.3) that allows us to express  $\langle N_+ \rangle_{\text{asym}}$  by  $\langle N_+ \rangle_{A=0}$  and  $A$ . Multiplying both sides of Eq. (2.4) by  $\cos(2\varphi)$  and integrating over an available phase space, assuming  $A \ll 1$  such that  $(1 \pm A)^{-1} \approx 1 \mp A$  and neglecting the  $A^2$  terms, we obtain

$$\langle v_2^+ \rangle_A \approx \langle v_2^+ \rangle_{A=0} - \alpha A \left[ \langle v_2^+ \rangle_{A=0} - \langle v_2^+ \rangle_{\text{asym}} \right], \quad (2.5)$$

and

$$\langle v_2^- \rangle_A \approx \langle v_2^- \rangle_{A=0} + \alpha A \left[ \langle v_2^- \rangle_{A=0} - \langle v_2^- \rangle_{\text{asym}} \right], \quad (2.6)$$

where  $\langle v_2^{\pm} \rangle_A$  denotes elliptic flow at a given value of  $A$ , and  $\langle v_2^{\pm} \rangle_{\text{asym}}$  represents an average elliptic flow of particles responsible for a non-zero value of  $A$ . The elliptic flow for all events with  $A = 0$  is denoted by  $\langle v_2^{\pm} \rangle_{A=0}$ .

As is evident from the above equations, a linear dependence on  $A$  is expected naturally only if the elliptic flow of particles contributing to a non-zero asymmetry differs from the elliptic flow of particles leading to  $A = 0$ . In the next section, we discuss two mechanisms that naturally lead to  $\langle v_2 \rangle_{A=0} > \langle v_2 \rangle_{\text{asym}}$ , being qualitatively consistent with the preliminary data.

<sup>1</sup> So that we can expand all variables around  $A = 0$ .

<sup>2</sup> If the same particles are used to calculate  $A$  and  $\langle N_{\pm} \rangle_A$ , then  $\alpha \simeq 1$ . In the STAR measurement,  $\langle N_{\pm} \rangle_A$  and  $A$  are calculated from similar sets of particles, but not identical ones. This distinction may engender a value that differs slightly from 1.

<sup>3</sup> To obtain  $A = 0.1$ , for example, we could increase  $N_+ - N_-$ , or/and decrease  $N_+ + N_-$ . Thus, for larger values of  $A$ ,  $N_+ + N_-$  is expected to decline as a function of  $A$ . We verified this in our simple model discussed in the next section, where  $\beta \approx 2.3$ , and  $\alpha = 0.96$ .

### III. TWO MECHANISMS

In this section, we discuss two mechanisms that offer qualitative and partly quantitative agreement with the preliminary STAR data.

From various measurements of the balance function in rapidity, we know that electric charges balance each other with a characteristic distance between the charges of about 0.5 unit of rapidity [21]. This finding is confirmed successfully in the hydrodynamic model with locally conserved charge production at freeze-out [19, 20].<sup>4</sup> Consequently, a pair of pions with opposite charges originating from a fluid element or a resonance, create a non-zero  $A$  in a given rapidity window provided that one pion is produced inside of this window and the other outside it. If both charges are produced inside a bin they do not contribute to  $N_+ - N_-$ . In the STAR experiment, the elliptic flow is measured in  $|\eta| < 1$  that is broader than the typical width of the balance function.

In Fig. 1, we schematically depict the first mechanism, leading to Eq. (1.2). Fluid elements and resonances, in short clusters, located close to  $\eta = 0$  usually produce both pions inside the pseudorapidity window. Only clusters located close to  $|\eta| = 1$  typically create a non-zero asymmetry parameter. From the PHOBOS data [22], we know that elliptic flow of charged particles as a function of pseudorapidity can be roughly described as  $v_2(\eta) \sim 1 - |\eta|/6$  (further discussed in section 5). Thus, clusters located close to  $|\eta| = 1$  have smaller elliptic flow compared to clusters located close to  $\eta = 0$ . Consequently, the elliptic flow of pairs responsible for a non-zero asymmetry is smaller than that of pairs leading to  $A = 0$ . Using Eq. (1.2) we conclude that  $\langle v_2^+ \rangle_A$  decreases and  $\langle v_2^- \rangle_A$  increases as a function of  $A$ .<sup>5</sup>

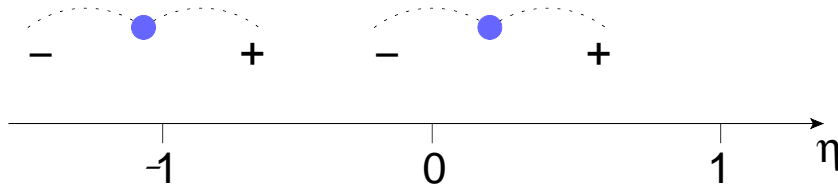


FIG. 1: Clusters (resonances, fluid elements), denoted by the blue dots, positioned close to  $\eta = 0$ , decay into final particles located inside the rapidity bin  $|\eta| < 1$  and clearly cannot create a non-zero asymmetry,  $A$ . Only clusters located close to the boundary can produce one pion inside and one pion outside of our rapidity bin. From the PHOBOS data, we know that elliptic flow is slightly smaller away from  $\eta = 0$ . Consequently, the elliptic flow of particles creating the asymmetry,  $A \neq 0$ , is smaller than that of particles leading to zero asymmetry,  $A = 0$ .

The second mechanism is explicitly related to the late locally conserved charge production in the hydrodynamic picture, see Fig. 2. Clusters with small transverse momentum

<sup>4</sup> In contrast to models with an initial charge creation (such as UrQMD) that cannot describe the experimental data on the balance function [21].

<sup>5</sup> By selecting events with  $A > 0$ , for example, we trigger configurations wherein positive pions are inside a rapidity window and the negative ones are outside it. In this way, we add positive particles with small  $v_2$  and, effectively, the  $v_2$  for positive particles is lowered. Since the number of negative particles with a small  $v_2$  is reduced, thus effectively, their  $v_2$  is increased.

(resonances) or small transverse velocity (fluid elements) usually decay into pairs of pions with a large rapidity separation (a broad balance function). In contrast, clusters with large transverse momentum or velocity engender a small rapidity separation (a narrow balance function). Undoubtedly, clusters with a broad balance function are more likely to produce a non-zero charge asymmetry parameter,  $A$ . On the other hand, we know that the elliptic flow of clusters with a small transverse momentum (velocity) is less than that of clusters with a high transverse momentum, e.g., [3]. Consequently  $\langle v_2 \rangle_{\text{asym}}$  is smaller than  $\langle v_2 \rangle_{A=0}$ , so leading to the linear dependence of  $\langle v_2^- \rangle_A - \langle v_2^+ \rangle_A$  on  $A$ .

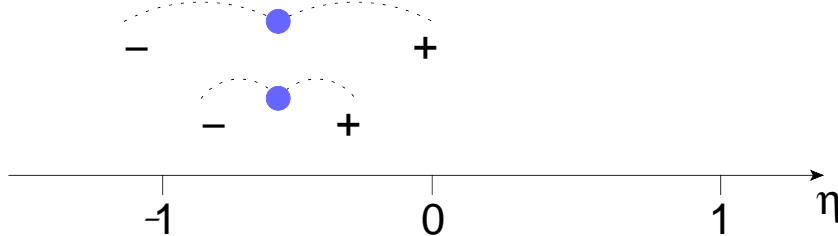


FIG. 2: Clusters (resonances, fluid elements), denoted by the blue dots, with low transverse momentum (velocity) produce particles separated more in rapidity compared to clusters with high transverse momentum. Consequently, non-zero values of  $A$  are mainly driven by clusters with a small  $p_t$  that are characterized by a small  $v_2$ . Thus, the elliptic flow of particles creating asymmetry,  $A \neq 0$ , is smaller than that of particles leading to zero asymmetry,  $A = 0$ .

To quantify these effects, we undertook a simplified Monte Carlo calculation.<sup>6</sup> As shown in Fig. 3, the signal we obtained is of the same order-of-magnitude as the data. In fact, we obtained  $r \approx 0.02$ , see Eq. (1.2), that is only a factor of 1.5 smaller than the preliminary STAR data,  $r_{\text{exp}} \approx 0.03$ . In our calculation, both  $A$  and  $v_2$  are calculated for particles in  $|\eta| < 1$ . However, we note that our results represent only an order-of-magnitude estimate, and more advanced calculations are required to draw definite conclusions.

We checked that the effect schematically presented in Fig. 1 is responsible approximately for 35% of the signal shown in Fig. 3. We also checked that calculating  $v_2$  in  $|\eta| < 0.2$  and  $A$  in  $|\eta| < 1$  reduces our final results by about 10%. However, when calculating  $v_2$  in  $|\eta| < 1.5$ , and  $A$  in  $|\eta| < 1$ , we obtained a significantly smaller value,  $r \approx 0.006$ . Taking  $v_2$  in  $|\eta| < 2$  and  $A$  in  $|\eta| < 1$  lowers our results approximately by a factor of 10. Finally, we mention

<sup>6</sup> In each event, we sampled clusters from the Poisson distribution with an average number of clusters,  $\langle N_c \rangle = 570$ . All clusters were uniformly distributed in pseudorapidity over  $|\eta| < 3$  and in transverse momentum according to the thermal distribution,  $e^{-2p_t/\langle p_t \rangle}$  with  $\langle p_t \rangle = 0.7$  GeV. A cluster with a given  $\eta$  and  $p_t$  decays into two oppositely charged particles, located symmetrically around  $\eta$ . The pseudorapidity distance between them is sampled from the Gaussian distribution with its standard deviation  $\sigma = 1/(1 + p_t/\langle p_t \rangle)$ , so that for a cluster with  $p_t = \langle p_t \rangle$ ,  $\sigma = 0.5$ . This dependence on  $p_t$  approximately agrees with a rho meson decay at a given  $p_t$  into two pions. Finally, we sampled the azimuthal angles of the two particles using  $1 + 2v_2(p_t, \eta) \cos(2\varphi)$  with  $v_2(p_t, \eta)$  given by  $0.04(1 - |\eta|/6)p_t/\langle p_t \rangle$  for  $p_t < 2$  GeV, and  $0.04(1 - |\eta|/6)2/\langle p_t \rangle$  for  $p_t > 2$  GeV.  $A$  and  $v_2$  are calculated for particles in  $|\eta| < 1$ . In our calculation we obtained  $\langle v_2 \rangle \approx 0.036$ , and approximately 380 charged particles in the midrapidity region  $|\eta| < 1$ , approximately agreeing with 200 GeV Au+Au collisions in the 30 – 40% centrality class.

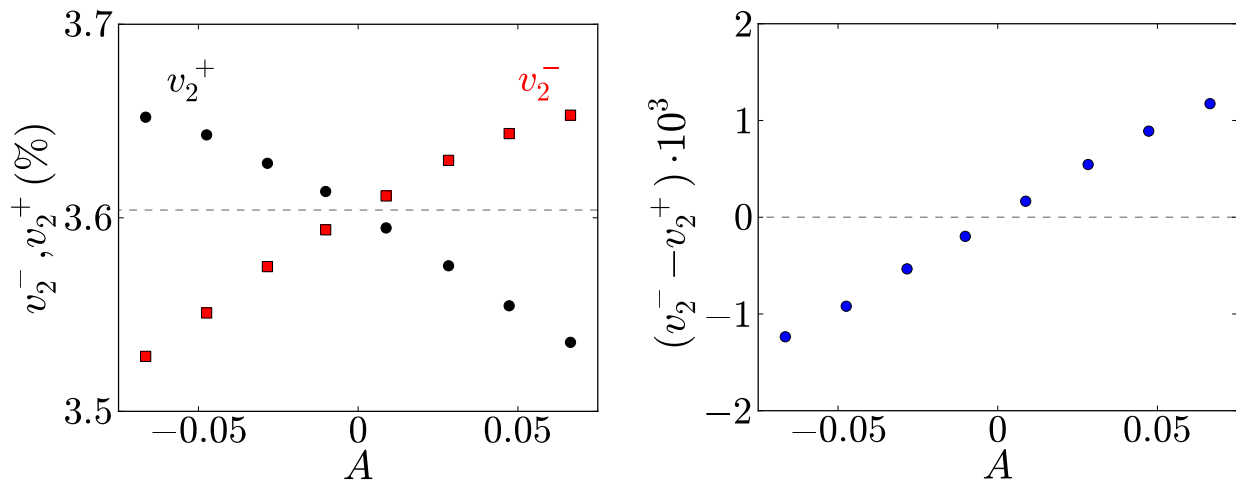


FIG. 3: Our results for the elliptic flow coefficient for positive and negative particles as a function of asymmetry parameter  $A = (N_+ - N_-)/(N_+ + N_-)$ . In our simplified model we obtain  $r \approx 0.02$ , see Eq. (1.2), to be compared with the preliminary STAR data  $r_{\text{exp}} \approx 0.03$ . Note that our results represent only an order-of-magnitude estimate.

that in our simplified analysis we neglected experimental cuts in the transverse momentum which may slightly modify our numbers.

It would be desirable to perform a more realistic calculations in an event-by-event 3 + 1-dimensional hydrodynamic model, wherein the effect presented in Fig. 2 is naturally present. This problem is discussed in the next section.

#### IV. HYDRODYNAMIC CALCULATION

The collective flow in heavy-ion collisions can be reproduced satisfactory within relativistic hydrodynamics [1–3]. Statistical emission and resonance decay at freeze-out account for part of the observed charge balancing correlations. Additionally, local charge balancing in particle production [18] can be included in the event generator [20], yielding the right qualitative description of the one- and two-dimensional charge dependent correlations. We used a 3 + 1-dimensional hydrodynamic model with statistical emission at freeze-out including the local charge conservation mechanism and resonance decays [23]. In order to study non-flow correlations, particle emission from the freeze-out hypersurface should be done via Monte-Carlo event generation. The default implementation of the statistical emission in THERMINATOR [24] generates primordial particles with the Poisson distribution for each type of particle. In the present calculation, we fix the total charge produced in the fireball, for simplicity fixing the multiplicities for all particles emitted from the fireball in each event. The charge asymmetry measured in a limited acceptance window mainly is due to the separation of an unlike charged pair as described in the previous section.

The statistical emission code [24] follows resonance decays, and such charge correlations are realistically described in the model. Together with the effects of local charge conservation, correlating the emission of primordial particles, it yields a good quantitative description of charge balance functions in semi-central Au-Au collisions [23]. To study the weak charge

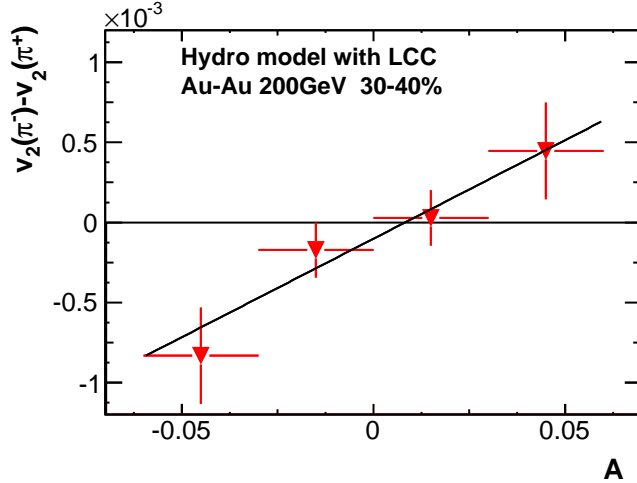


FIG. 4: The charge asymmetry dependence of  $\pi^+$  and  $\pi^-$  elliptic flow coefficients in the hydrodynamic model followed by statistical emission with local charge conservation. We obtained  $r = 0.012 \pm 0.004$  compared with the preliminary STAR data,  $r_{\text{exp}} \approx 0.03$ .

splitting signal, a large statistics is required. We generated  $10^6$  events for the centrality 30-40% wherein the measured signal is the strongest, and where the hydrodynamic model agrees best with the data on charge balance functions. The elliptic flow,  $v_2$ , for  $\pi^+$  and  $\pi^-$  is calculated for events with different charge asymmetry in the interval  $|\eta| < 1$ , using two subevents with a pseudorapidity separation  $|\Delta\eta| > 0.3$  to define  $v_2$ , following the experimental procedure [8]. The Monte-Carlo calculation with local charge conservation and resonance decays exhibits the expected signal, viz., a decrease of  $v_2(\pi^+)$  and an increase of  $v_2(\pi^-)$  with the charge asymmetry  $A$  in the event (Fig. 4). The slope parameter,  $r \simeq 0.012$ , is about one half of the observed magnitude. We note that the pseudorapidity dependence of the elliptic flow  $v_2(\eta)$  observed experimentally [22] is noticeably underestimated in 3 + 1-dimensional hydrodynamic simulations [23, 25]. The steeper pseudorapidity dependence of  $v_2$  is expected to improve the agreement between the calculated charge splitting of the elliptic flow with the experimental findings. In the next section, we comment further on this issue.

Finally, we discuss the centrality dependence of the signal. Two effects that are not well controlled in hydrodynamic models may cause the decrease of the slope parameter for peripheral events. First, the balance function in pseudorapidity is widening for peripheral events. Second, for peripheral events, correlations due to elliptic flow are diluted by the larger contribution of particles emitted from the nonthermal corona in the interaction region, while the charge asymmetry acquires contributions both from the core and the corona.

## V. COMMENTS AND CONCLUSIONS

Several comments are warranted.

(i) In this paper we discussed two mechanisms leading to elliptic flow splitting as a function of the asymmetry parameter,  $A$ . We note that we expect a similar effect for higher

harmonics,  $v_n$ . In particular, for the triangular flow

$$\langle v_3^- \rangle_A - \langle v_3^+ \rangle_A \sim A, \quad (5.1)$$

although the signal is expected to be significantly weaker in comparison to the case for  $v_2$ . We expect that  $r$ , see Eq. (1.2), should be smaller roughly by a factor of  $\langle v_2 \rangle / \langle v_3 \rangle \approx 3$  [26]. This problem will be discussed elsewhere.

(ii) The key ingredient in our analysis is the assumption of local charge conservation at freeze-out. In this scenario, particle pairs with higher momentum are more strongly collimated in rapidity than are pairs with smaller momentum, see Fig. 2. This allows us to understand the centrality dependence of the rapidity balance function [21], in contrast to models with initial charge creation (such as UrQMD). Consequently, in models without late local charge conservation we do not expect to observe the elliptic flow splitting discussed in this paper.

(iii) According to the PHOBOS data, the elliptic flow of charged particles in the midrapidity region changes significantly as a function of pseudorapidity [22]. However, the results of the STAR Collaboration indicate that elliptic flow in the midrapidity region weakly depends on  $\eta$  [27], so being consistent with hydrodynamic calculations (see section 4). Consequently, the mechanism presented in Fig. 1 may be suppressed if we take the STAR data into account. However, this is not a problem because, as we discussed in section 3, this mechanism is responsible for only 25% of the measured signal, and 35% of the signal presented in Fig. 3.

In conclusion, we studied the dependence of the elliptic flow coefficients for positive and negative particles as a function of the event-by-event charge asymmetry parameter. Recently, this phenomenon was interpreted as evidence of the chiral magnetic wave. In this paper, we argued that the origin of this effect may be less exotic and actually is consistent with the hydrodynamic picture of heavy-ion collisions with late local charge conservation.

We argued that particle pairs leading to a non-zero asymmetry parameter,  $A \neq 0$ , are characterized by a smaller elliptic flow in contrast to particle pairs resulting in  $A = 0$ . We showed that this fact alone is sufficient to qualitatively explain the preliminary STAR data, in particular, a linear dependence of  $\langle v_2^- \rangle_A - \langle v_2^+ \rangle_A$ , as a function of  $A$ . Our quantitative results, based on a simplified Monte Carlo estimation and the state of the art 3+1-dimensional hydrodynamic model calculations, are in agreement, within a factor of 2, with the preliminary STAR data.

## Acknowledgments

We thank H.-U. Yee for interesting discussions. Remarks by V. Koch and L. McLerran are highly appreciated. W. Broniowski graciously helped us in modifying the THERMINATOR code. A.B. is supported through the RIKEN-BNL Research Center. The work is partly supported by the National Science Centre, Poland, grant DEC-2012/05/B/ST2/02528.

---

[1] J. -Y. Ollitrault and F. G. Gardim, arXiv:1210.8345 [nucl-th].



- [2] U. W. Heinz and R. Snellings, arXiv:1301.2826 [nucl-th].
- [3] C. Gale, S. Jeon and B. Schenke, Int. J. of Mod. Phys. A, Vol. 28, **1340011** (2013) [arXiv:1301.5893 [nucl-th]].
- [4] B. Mohanty [STAR Collaboration], J. Phys. G **38**, 124023 (2011) [arXiv:1106.5902 [nucl-ex]].
- [5] J. C. Dunlop, M. A. Lisa and P. Sorensen, Phys. Rev. C **84**, 044914 (2011) [arXiv:1107.3078 [hep-ph]].
- [6] J. Steinheimer, V. Koch and M. Bleicher, Phys. Rev. C **86**, 044903 (2012) [arXiv:1207.2791 [nucl-th]].
- [7] J. Xu, L. -W. Chen, C. M. Ko and Z. -W. Lin, Phys. Rev. C **85**, 041901 (2012) [arXiv:1201.3391 [nucl-th]].
- [8] H. Ke [STAR Collaboration], J. Phys. Conf. Ser. **389**, 012035 (2012) [arXiv:1211.3216 [nucl-ex]].
- [9] G. Wang [STAR Collaboration], arXiv:1210.5498 [nucl-ex].
- [10] J. M. Campbell, J. C. Dunlop, M. A. Lisa and P. Sorensen, poster at Quark Matter 2012.
- [11] M. Bleicher, E. Zabrodin, C. Spieles, S. A. Bass, C. Ernst, S. Soff, L. Bravina and M. Belkacem *et al.*, J. Phys. G **25**, 1859 (1999) [hep-ph/9909407].
- [12] Z. -W. Lin, C. M. Ko, B. -A. Li, B. Zhang and S. Pal, Phys. Rev. C **72**, 064901 (2005) [nucl-th/0411110].
- [13] D. E. Kharzeev and H. -U. Yee, Phys. Rev. D **83**, 085007 (2011) [arXiv:1012.6026 [hep-th]].
- [14] Y. Burnier, D. E. Kharzeev, J. Liao and H. -U. Yee, Phys. Rev. Lett. **107**, 052303 (2011) [arXiv:1103.1307 [hep-ph]].
- [15] Y. Burnier, D. E. Kharzeev, J. Liao and H. -U. Yee, arXiv:1208.2537 [hep-ph].
- [16] D. E. Kharzeev, L. D. McLerran and H. J. Warringa, Nucl. Phys. A **803**, 227 (2008) [arXiv:0711.0950 [hep-ph]].
- [17] A. Bzdak, V. Koch and J. Liao, arXiv:1207.7327 [nucl-th].
- [18] S. Jeon and S. Pratt, Phys. Rev. C **65**, 044902 (2002)
- [19] S. Schlichting and S. Pratt, Phys. Rev. C **83**, 014913 (2011) [arXiv:1009.4283 [nucl-th]].
- [20] P. Bożek and W. Broniowski, Phys. Rev. Lett. **109**, 062301 (2012)
- [21] M. M. Aggarwal *et al.* [STAR Collaboration], Phys. Rev. C **82**, 024905 (2010) [arXiv:1005.2307 [nucl-ex]].
- [22] B. Alver *et al.* [PHOBOS Collaboration], Phys. Rev. Lett. **98**, 242302 (2007) [nucl-ex/0610037].
- [23] P. Bożek, Phys. Rev. C **85**, 034901 (2012)

- [24] M. Chojnacki, A. Kisiel, W. Florkowski and W. Broniowski, *Comput. Phys. Commun.* **183**, 746 (2012)
- [25] B. Schenke, S. Jeon and C. Gale, *Phys. Rev. C* **85**, 024901 (2012)
- [26] A. Adare *et al.* [PHENIX Collaboration], *Phys. Rev. Lett.* **107**, 252301 (2011) [arXiv:1105.3928 [nucl-ex]].
- [27] B. I. Abelev *et al.* [STAR Collaboration], *Phys. Rev. C* **77**, 054901 (2008) [arXiv:0801.3466 [nucl-ex]].